

CALCULATION OF THE ASYMPTOTIC CRACK TIP FIELDS FOR A DYNAMIC
CRACK GROWTH IN DUCTILE-POROUS SOLIDS

B. Potthast and K.P. Herrmann*

In this paper, the asymptotic crack tip fields for fast running cracks in pressure sensitive, ductile-porous solids are determined. For the constitutive description of pressure sensitive porous solids, reference is made to the Tvergaard/Needleman yield criterion (1), (2) with an associative flow law which is an extended version of the Gurson model. Crack tip fields in solids show a singular behaviour at the crack tip. The strength of this singularity depends in a dominant manner on the material behaviour as well as on the crack tip velocity as it was already shown by Achenbach et al (3) and Herrmann and Potthast (4). Therefore, the second focus is to quantify the singular behaviour of the crack tip fields for different material parameters and crack tip velocities.

INTRODUCTION AND MATERIAL LAW

A focus of this paper is a characterization of the model parameters in view of their influences on the crack tip fields. For that purpose the material model of Tvergaard/Needleman is transferred to the elastic-plastic model of a crack tip surroundings of a stationary growing crack. The solutions are assumed to be of a variable separable form with a radial singular behaviour. The asymptotic stress- and velocity crack tip fields are numerically obtained by using the incremental theory, a stationary crack growth, plane stress conditions and mode I-loading. Studies concerning pressure sensitive porous materials and quasistatic crack growth have been performed by Radi and Bigoni (5).

For the mathematical description of the problem, we adopt a yield criterion by Tvergaard/Needleman. This isotropic/kinematic hardening criterion

$$\Psi^{(TN)} = \frac{3}{2} \frac{b_{ij} b_{ij}}{\sigma_f^2} + 2q_1 f \cosh\left(\frac{q_2}{2} \frac{\beta_{kk}}{\sigma_f}\right) - (1 + (q_1 f)^2) = 0 \quad (1)$$

represents a yield criterion for pressure sensitive materials containing a void volume

* Laboratorium für Technische Mechanik, Paderborn University.

fraction f , which is assumed to be constant. Therefore growth and nucleation of voids has been neglected. According to experimental results the pressure sensitive behaviour following from the porosity is treated in the mid term of eq. (1). For simplicity the additional quantifying parameters q_1, q_2 are set equal to one. The stress σ_F describes the radius of the actual yield surface of the matrix material and is given by

$$\sigma_F = (1 - b)\sigma_Y + b\sigma_E \quad (2)$$

where σ_Y and σ_E are the initial and the actual yield stress of the matrix material. The mixed or kinematic hardening parameter $b \in [0, 1]$ describes the portion of kinematic hardening. The hardening is pure isotropic if $b=1$ and pure kinematic if $b=0$. The stress tensor b_{ij} denotes the deviatoric part of $\beta_{ij} = \sigma_{ij} - \alpha_{ij}$, where α_{ij} denotes the back stress tensor. Following references (1), (2) as well as eq. (1) the necessary evolution law for σ_F can be stated as

$$\dot{\sigma}_F = b\dot{\sigma}_E \quad (3)$$

If $\dot{\epsilon}_E^{(p)}$ denotes the effective plastic strain rate, then the macroscopic plastic strain rate $\dot{\epsilon}_{ij}^{(p)}$ is assumed to be related to $\dot{\epsilon}_E^{(p)}$ by

$$\beta_{ij} \dot{\epsilon}_{ij}^{(p)} = (1 - f)\sigma_F \dot{\epsilon}_E^{(p)} \quad (4)$$

Assuming a bilinear material behaviour of the matrix material, the relation between the effective plastic strain rate and the actual yield stress of the matrix material becomes

$$\dot{\epsilon}_E^{(p)} = \frac{E - E_t}{EE_t} \dot{\sigma}_E \quad (5)$$

where ν denotes Poisson's ratio, E the young's modulus and E_t the tangent modulus in the uniaxial tensile test. Furthermore the Prager consistency must be fulfilled. Therefore,

$$\frac{\partial \Psi}{\partial \sigma_{ij}} \dot{\sigma}_{ij} + \frac{\partial \Psi}{\partial \alpha_{ij}} \dot{\alpha}_{ij} + \frac{\partial \Psi}{\partial \sigma_F} \dot{\sigma}_F = 0 \quad (6)$$

must be fulfilled. For the presented material law, the basic equations of the continuum mechanics, which consist of the well known equations of motion and the associative incremental strain decomposition

$$\dot{\epsilon}_{ij} = \dot{\epsilon}_{ij}^{(e)} + \dot{\epsilon}_{ij}^{(p)} \quad , \quad \dot{\epsilon}_{ij}^{(p)} = \left\{ \frac{1}{h} \frac{\partial \Psi}{\partial \sigma_{ij}} \left(\frac{\partial \Psi}{\partial \sigma_{kl}} \dot{\sigma}_{kl} \right) \right\} \quad \text{or} \quad \dot{\epsilon}_{ij}^{(p)} = \Lambda \frac{\partial \Psi}{\partial \sigma_{ij}} \quad (7)$$

have been adopted, with Λ as the plastic multiplier.

It is recognizable, that the governing equations of the crack problem consist of a family of partial differential equations. Thereby the dot denotes the material time differentiation. Regarding the derivations of the yield criterion (eqs. (6), (7)), the relation $\Lambda = \sigma_f \lambda$ and the evolution law for the back stress tensor

$$\dot{\alpha}_{ij} = \mu \lambda \beta_{ij} \quad , \quad (8)$$

then the plastic multiplier λ becomes

$$\lambda = \frac{\frac{\partial \psi}{\partial \sigma_{ij}} \dot{\sigma}_{ij}}{\frac{\partial \psi}{\partial \sigma_{kl}} \beta_{kl} \left(\mu + \frac{C}{\sigma_f} \frac{\partial \psi}{\partial \sigma_{mn}} \beta_{mn} \right)} \quad , \quad \mu = \frac{C}{\sigma_f} \frac{\partial \psi}{\partial \sigma_{ij}} \beta_{ij} \left(\frac{1}{b} - 1 \right) \quad (9)$$

For the evaluation of eq. (9) a coincidence between the models of Gurson and Tvergaard/Needleman for proportional stress histories has to be assumed.

CRACK PROPAGATION AND ASYMPTOTIC ANALYSIS

It is assumed in an asymptotic analysis that the near tip fields consist of plastic and elastic unloading angular regions. The crack tip region of a propagating crack with the velocity v under Mode I loading conditions exhibits a first plastic region in front of the crack tip which is surrounded by an elastic region. The second plastic region exists along the crack surfaces. In order to specify the characteristic behaviour of the stress- and displacement rate fields in the vicinity of the crack tip for a plane stress state and dynamic crack growth, characteristic separable asymptotic first order base functions for the stresses σ_{ij} , α_{ij} and the displacement rates \dot{u}_i in r and θ of the form $f(\theta) = g(\theta) r^s$ are introduced.

The asymptotic base functions offer the advantage to reduce the partial differential equation system to an ordinary differential equation system independent of the distance r to the crack tip (Fig. 1). The constitutive equations and the asymptotic functions are transferred to the crack tip surroundings. Therefore, the resulting equations for the Tvergaard/Needleman ^(TN) model can be summarized in first-order systems of non-linear ordinary differential equations

$$f_k^{(TN)}(U'_i, U_i, \Sigma'_F, \Sigma_F, \Sigma'_{ij}, \Sigma_{ij}, A'_{ij}, A_{ij}) = 0 \quad , \quad \begin{cases} k = 9 & \text{for plane stress} \\ k = 11 & \text{for plane strain} \end{cases} \quad (10)$$

respectively, where Σ_{ij} , Σ_F , A_{ij} , \dot{U}_i are the stress and displacement rate functions of θ only. On account of the structure of the equation systems, eq. (10) is integrated numerically over the crack tip variable θ . Due to the symmetry of the mode I-crack problem, the integration range of the differential equation system can be reduced to the interval $\theta = [0; \pi]$. The specification of the differential equation system is performed by formu-

lating the boundary conditions for $\theta = 0$, $\theta = \pi$ and the transition conditions between the elastic and plastic regions.

Elastodynamic crack tip fields

The formulated differential equation systems in the last chapter are valid for the elastic-plastic regions $\theta \in [0; \theta_{pl}]$, $\theta \in [\theta_{el}; \pi]$ of the crack tip surroundings only. For the elastic region the solution of the near tip fields follows from (3). For that purpose the displacement rate potentials

$$\frac{\partial \dot{\phi}}{\partial x_1} + \frac{\partial \dot{\psi}}{\partial x_2} = \dot{u}_1 \quad , \quad \frac{\partial \dot{\phi}}{\partial x_2} - \frac{\partial \dot{\psi}}{\partial x_1} = \dot{u}_2 \quad (11)$$

are introduced, in which $\dot{\phi}$ and $\dot{\psi}$ are solutions of the wave equations

$$\dot{\phi}_{,ii} = \frac{1}{C_L^2} \ddot{\phi} \quad , \quad \dot{\psi}_{,ii} = \frac{1}{C_T^2} \ddot{\psi} \quad (12)$$

The potentials are connected with the displacement rates through the equations of motion and the incremental Hooke's law. In eq. (12) C_L and C_T denote the longitudinal and transverse elastic wave speeds. For solutions $\dot{\phi}$ and $\dot{\psi}$ of the separable asymptotic form in r and θ , an analogous ordinary differential equation system like in eq. (10) can be installed for the elastic region. The consequence is to design a whole integration scheme for the integration range $\theta \in [0; \pi]$ which distinguishes between the plastic and elastic regions automatically.

FORMULATION OF THE BOUNDARY VALUE PROBLEM

The specification of the differential equation system is performed by formulating the boundary values for $\theta = 0$, $\theta = \pi$ and the transition conditions as well as the transition values between the elastic and plastic regions for the unknown angles $\theta = \theta_{pl}$, $\theta = \theta_{el}$ (Fig. 1). Regarding a bilinear material behaviour the first transition $\theta = \theta_{pl}$ occurs if the plastic part of eq. (7) vanishes. This implies that

$$\frac{\partial \dot{\psi}}{\partial \sigma_{kl}} \dot{\sigma}_{kl} = 0 \quad (13)$$

causes the first transition. The calculation of the second transition is not determined by an analogous condition to eq. (13) only. The model of Tvergaard/Needleman describes isotropic and kinematic hardening. Therefore, the angle $\theta = \theta_{el}$ for a second yielding depends on the stresses $\alpha^{(TN)}(r_{pl}, \theta_{pl})$, $\sigma_r^{(TN)}(r_{pl}, \theta_{pl})$ and the additional condition for the transition for Tvergaard/Needleman's model leads to

$$\psi^{(TN)}(\sigma_{ij}(r, \theta), \alpha_{ij}(r_{pl}, \theta_{pl}), \sigma_r(r_{pl}, \theta_{pl})) = 0 \quad (14)$$

A second yielding takes place if the actual stresses $\sigma_{ij}(r, \theta)$ fulfil the yield criterion (14). This criterion leads to the second transition angle θ_{c2} . The boundary values apply zero stresses of the crack surfaces for $\theta = \pi$ and the symmetry of the near crack tip fields due to a mode I-loading situation (4). The calculation of the boundary values for the stresses σ_{ij} , the back stress tensor α_{ij} and the radius of the actual yield surface of the matrix material σ_f follows from the equation of motion, the incremental stress-strain equation, the corresponding yield criterion and the evolution laws of eqs. (1) and (2).

NUMERICAL RESULTS

The numerical values of the singularity exponent s for plane stress conditions are given in Fig. 2 for selected values of $\alpha^* = E_t/E$ and $\nu = 0.3$. This figure shows that if the crack speed is less than approximately $\beta_t = v \sqrt{\rho/E_t} < 0.3$, then the order of the singularity does not differ significantly from that for quasistatic conditions independent of the material model. In addition, the results of the singularity exponent are very sensitive to the ratio $\alpha^* = E_t/E$ of the bilinear stress-strain relation which has been shown in references (3), (4). The pressure sensitivity parameter μ^* as well as the mixed hardening parameter b substantially changes the level of the singularity exponent s , whereas the exponential behaviour of $s(\beta_t)$ remains. Plots of the angle dependent stress fields for $\alpha^* = 0.5$ of the $(^{TN})$ -model are shown in Fig. 3 and 4. The curves are normalized such that $\Sigma_{22}(\theta = 0) = 1$. The calculations are compared with known elastic solutions and quasi-static solutions of elastic-plastic materials from the literature. The representations of the stresses show a significant dependence on the crack tip velocity for $\beta_t > 0.3$, a lower mixed hardening coefficient $b = 0.5$ reduces the differences a few.

REFERENCES

- (1) Tvergaard, V. „Influence of voids on shear band instabilities under plain strain conditions“, Int. J. Fracture, Vol. 17, 1981, pp. 389-407.
- (2) Tvergaard, V. „Material failure by void coalescence in localized shear bands“, Int. J. Solids Struct., Vol. 18, 1982, pp. 659-672.
- (3) Achenbach, J.D. and Kanninen, M.F. and Popelar, C.H. „Crack-tip fields for fast fracture of an elastic-plastic material“, J. Mech. Phys. Solids, Vol. 29, 1981, pp. 211-225.
- (4) Herrmann, K.P. and Potthast, B. „Ermittlung fließbruchmechanischer Kenngrößen für dynamische Rißprobleme in elastoplastischen Mehrkomponentenmedien“, DFG-Report, 1995.
- (5) Radi, E. and Bigoni, D. „Effects of anisotropic hardening on crack propagation in porous-ductile materials“, J. Mech. Phys. Solids, Vol. 44, 1996, pp. 1475-1508.

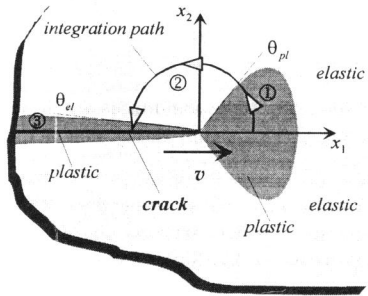


Figure 1 Crack tip surroundings of a dynamically propagating crack

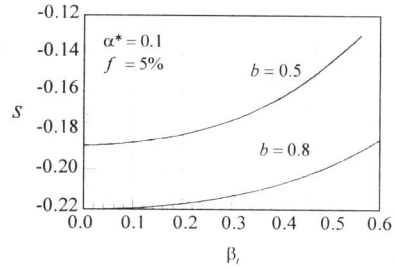


Figure 2 Exponent $s(\beta_i)$ of the crack tip singularity for the T/N model

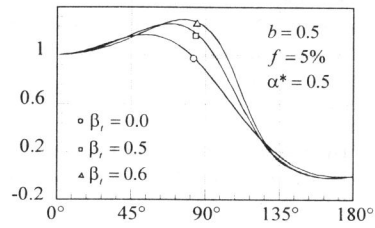
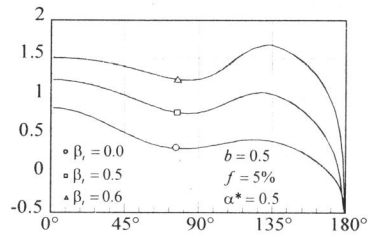
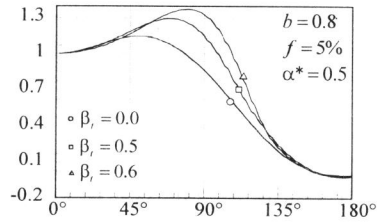
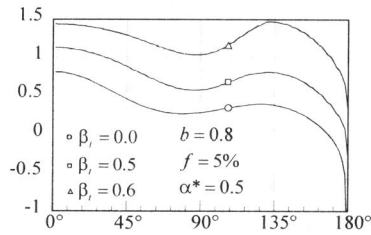


Figure 3 Stress fields $\Sigma_{11}(\theta)$

Figure 4 Stress fields $\Sigma_{22}(\theta)$